Negative refraction and focusing of elastic Lamb waves at an interface

Suraj Bramhavar, Claire Prada, Alexei A. Maznev, Arthur G. Every, Theodore B. Norris, and Todd W. Murray

Phys. Rev. B **83**, 014106 — Published 24 January 2011

DOI: 10.1103/PhysRevB.83.014106

Negative Refraction and Focusing of Lamb Waves at an Interface

Suraj Bramhavar[1], Claire Prada[2], Alexei A. Maznev[3], Arthur G. Every[4], Theodore B. Norris[5], and Todd W. Murray[6]

[1] *Department of Electrical and Computer Engineering, Boston University, Boston, MA 02215*

[2] *Institut Langevin, CNRS UMR 7587, ESPCI ParisTech, 10 rue Vauquelin, 75231 Paris Cedex 05- France*

[3] *Department of Chemistry, Massachusetts Institute of Technology, Cambridge, MA 02139*

[4] *School of Physics, University of the Witwatersrand, PO Wits 2050, Johannesburg, South Africa*

[5] *Center for Ultrafast Optical Science, University of Michigan, 2200 Bonisteel Boulevard, Ann Arbor, Michigan 48109*

[6] *Department of Mechanical Engineering, University of Colorado at Boulder, Boulder, CO 80309*

Abstract

We study negative refraction and focusing of elastic waves in a simple mechanical system comprised of a free standing plate with a step change in thickness. A point focused and intensity modulated laser source is used to excite backward propagating Lamb waves on one side of the step, and the displacement field is probed using an optical interferometer. Conversion between forward and backward propagating modes at the interface leads to negative refraction, and we demonstrate for the first time the operation of a flat lens, similar to that predicted by Veselago in negative index media, for guided elastic waves in isotropic media. We propose that guided elastic waves provide a convenient and powerful experimental test bed for the study of negative index physics.

I. INTRODUCTION

There is growing interest in the development of novel materials for the control and manipulation of electromagnetic and acoustic waves. Materials which exhibit backward wave propagation, also referred to as negative index materials, have received considerable attention due in part to the fact that these materials display negative refraction and a variety of other non-intuitive physical effects.[1-4] Backward wave motion is broadly defined as wave motion in which the energy flux direction, as given by the Poynting vector, is antiparallel to the phase velocity direction or direction of motion of the individual wave fronts. The possibility of such motion was first discussed in the early twentieth century by Lamb in reference to vibration of mechanical systems.[5] Since this time, backward wave propagation has been reported in a variety of structures such as optical and acoustic metamaterials,[6-10] photonic and phononic crystals,[11-13] and optical and acoustic waveguides.[14-16]

It has long been known that guided elastic waves, or Lamb waves, in a homogeneous plate can display backward wave propagation.[16] In addition, interference effects between forward and backward propagating waves can lead to plate resonances in which Lamb waves have a finite phase velocity along the plate but vanishing group velocity. Such zero group velocity resonances have seen renewed interest recently and can potentially be used for accurate determination of the elastic properties of plates or dimensional changes.[17-19] Guided elastic waves in other structures such as rods and cylindrical shells,[15, 20] and multilayer thin films and coatings[21] can also exhibit backward wave motion and associated zero group velocity resonances. While the existence of backward

wave modes in acoustic waveguides is well established, the behavior of such modes at the interface between two media, one supporting backward waves and the other only forward waves at a particular frequency, has not been reported. In this letter, we study the refraction of backward propagating Lamb waves at an interface between a plate which supports a backward propagating mode at a given propagation frequency ω_1 and wave-number k_1 and a plate which supports a forward propagating mode at the same ω_1 and k_1. A focused and intensity modulated continuous wave laser source, serving as an ultrasonic point source, is used to excite Lamb waves in an isotropic elastic plate with a step change in thickness. When the modulation frequency is chosen such that forward and backward propagating modes on respective sides of the thickness step overlap in $\omega(k)$ space, mode conversion is observed and the backward propagating waves emitted from the point source on one side of the plate are seen convert to forward propagating waves which focus on the opposite side of the interface. We believe that this is the first time that such a "slab" lens, originally predicted by Veselago for negative index optical media,[1] has been demonstrated for guided waves in homogeneous, isotropic media. In addition, this simple mechanical system provides a powerful test bed for the study of negative-index physics.

II. VESELAGO LENS FOR LAMB WAVES

Lamb wave propagation in a free, isotropic, and infinite plate is described by the Rayleigh-Lamb dispersion equation, which provides a relationship between the wave-number and frequency of waves propagating along the plate with displacement components both in the direction of propagation and perpendicular to the plate

surface.[22,23] For a fixed excitation frequency, there exist a finite number of real wave-numbers, corresponding to propagating waves, and an infinite number of imaginary or complex wave-numbers corresponding to exponentially decaying or evanescent waves. The dispersion relation for the first few modes in an aluminum plate, with a longitudinal wave velocity of c_L = 6.42 mm/μs and a transverse wave velocity of c_T = 3.04 mm/μs, is shown in Fig. 1(a), where only the propagating modes are considered. The phase velocity is found through $v_p = \omega/k$, while the group velocity is given by $v_g = d\omega/dk$. The modes are labeled as symmetric (*S*) or antisymmetric (*A*) depending on the material displacement with respect to the mid-plane of the plate. With the exception of the lowest order antisymmetric (A_0) and symmetric (S_0) modes, each supported mode sees a cutoff frequency at $k = 0$ corresponding to longitudinal or shear thickness modes. For this material, and over the range of $\omega(k)$ space shown, backward wave propagation is seen in the mode labeled S_{2b} where, for small values of wave-number, a negative slope is observed. In this nomenclature, the modes are labeled with a numerical subscript giving the mode number and the subscript *b* indicates backward propagation. The S_{2b} branch, which extends from $k = 0$ to the point at which the slope of the curve goes to zero ($v_g = 0$), is classified as part of the S_2 mode and is indeed connected to this mode through a small imaginary loop in $\omega(k)$ space.[15] The existence of backward waves in a particular mode depends on the Poisson's ratio (ν) and all propagating modes, with the exception of the three lowest modes (A_0, S_0, and A_1), exhibit backward wave propagation over some range of ν.[24,25] Backward waves themselves stem from repulsion of adjacent, closely spaced modes of the same family (*S* or *A*) in the vicinity of $k = 0$.[14, 25]

In order to study mode conversion between forward and backward propagating modes, an aluminum plate with a step change in thickness was fabricated by masking one side of the sample and wet-etching the other, resulting in the profile depicted in Fig. 1(b). When Lamb waves associated with a given mode encounter an interface between two media, mode conversion can occur in the reflected and transmitted waves such that the elastic boundary conditions between the media, continuity of stress and displacement, are satisfied. Mode conversion across the interface is expected to be strong when the spatial overlap between the displacement fields associated with modes on each side of the interface are similar.

When a backward-propagating wave is converted into a forward-propagating wave upon refraction at an interface, the phenomenon of negative refraction occurs.[1-3] Moreover, when the wave-numbers on both sides of the interface are equal, the angle of refraction is equal in magnitude but opposite in sign to the incidence angle. As a result, rays originating from a point source on one side of the interface will converge in the symmetrically situated point on the other side, thus resulting in a geometrically perfect image. This "Veselago lens" effect was originally proposed for electromagnetic waves in the context of negative index materials;[1] however, the same concept[1,3] is equally applicable to waves of any nature, as long as the conversion between backward- and forward-propagating modes takes place and the wave-number magnitude is preserved.

Here we seek to achieve mode conversion between the backward propagating S_{2b} branch in the thin side of the plate and the forward propagating S_2 mode in the thick side, and the

thickness step was chosen such that dispersion curves of these two modes intersect at a particular frequency. The mode conversion takes place near the interface, and over a length scale on the order of the wavelengths of the associated modes. Outside of this zone, the Rayleigh-Lamb dispersion equation may be used to predict the modes supported by the plate on each side of the interface. The dispersion curves (only symmetric modes are shown) calculated for each side of a sample with thicknesses of h_1 = 131.7 μm and h_2 = 102.5 μm are shown in Fig. 1(c) and a zoomed in version of the overlap region is shown in Fig. 1(d), where the solid and dotted lines correspond to the regions of the plate with thickness h_1 and h_2, respectively. The modes are seen to intersect at a frequency of 28.0 MHz.

III. EXPERIMENTAL DETAILS

The experimental set-up is depicted in Fig. 2. Lamb waves were generated through the thermoelastic mechanism using an intensity modulated, continuous wave diode laser with an integrated electro-absorption modulator, and operating at a wavelength of 1550 nm. The modulator was driven by a sinusoidal wave form from a signal generator. The fiber coupled output was sent to an erbium doped fiber amplifier where the modulated beam was amplified to 3.5 W. The amplified output was then collimated and focused using a lens to a spot size of 25 μm (full width at half maximum) at the surface of the plate. The position of the excitation point on the plate surface was adjusted using a 2-axis computer controlled translation stage. The normal displacement of the plate surface was detected using a path-stabilized Michelson interferometer incorporating a 200 mW frequency doubled Nd:YAG laser. The signal beam of the interferometer was directed through a

long working distance microscope objective to the sample surface. Light reflected from the surface was collected, combined with the reference beam, and sent to the photodetector. The output of the photodetector was sent to a lock-in amplifier where the in-phase and quadrature components of the signal, with respect to a reference derived from the excitation laser drive signal, were recorded.

IV. RESULTS

The Lamb wave dispersion behavior on each side of the interface was characterized first. The detection laser was fixed 2.0 mm from the interface and the excitation laser, driven at ω_1, was scanned in 10 μm steps away from the detection point and parallel to the interface. At each excitation laser position, the in-phase and quadrature components of the normal displacement were recorded. The phase of each propagating Lamb wave is periodic as the excitation laser is translated with respect to the detector by the wavelength of a particular mode, and the wave-numbers of all propagating modes $k(\omega_1)$ were determined through a Fourier transform of the complex data. The magnitudes of the Fourier transforms of scans taken with the source and detector on the thick (pth_1) and thin (pth_2) sides of the interface at a frequency of 28.0 MHz are shown in Figs. 3(a) and 3(b), respectively. In each graph, the wave-number peaks corresponding to all supported modes are identified. We note that there are several smaller peaks which remain unidentified in these plots, and which may be associated with reflected waves from sample boundaries. Backwards wave propagation of the S_{2b} mode is evidenced by the presence of a spatial transform peak with negative wave-number in pth_2 (Fig. 3(b)), indicating this mode propagates with a negative phase velocity. The wavelength of the S_2

mode (598 μm) in *pth₁* nearly matches that of the S_{2b} mode in *pth₂* (612 μm) at this frequency. This experiment was repeated to determine $\omega(k)$ over the frequency range from 27.5 MHz to 28.5 MHz in intervals of 100 kHz. The plate thicknesses on each side of the interface were determined by minimizing the mean squared error between calculated and measured dispersion curves over this frequency range. These thicknesses were further confirmed, to within 2 μm, using through thickness pulse-echo ultrasound measurements. The experimental results for the S_2 mode in *pth₁* and S_{2b} mode in *pth₂* are shown in Fig. 1(d) (squares) alongside the theoretical dispersion curves calculated for the best fit plate thicknesses of h_1 = 131.7 μm and h_2 = 102.5 μm. The experimental results confirm the intersection of the modes, and the dispersion curves show general agreement with theory for these thicknesses.

Two-dimensional scans of the displacement field were performed to evaluate the mode conversion at the interface. The detection laser was positioned 2.0 mm from the interface on *pth₁*. The excitation laser modulation frequency was fixed at 28.0 MHz. Taking the detection point as the origin (0,0) and referring to the coordinate system in Fig. 2, the generation laser was scanned from -2.5 mm to 2.5 mm in the *x*-direction (parallel to the interface) and 1.25 mm to 7.5 mm in the *y*-direction (perpendicular to the interface), both with a step size of 50 μm. The in-phase and quadrature displacement components were measured at each step. The excitation source was scanned rather than the detection point to ensure constant light collection, and hence detection sensitivity, over the scan. However, through the reciprocity principle, this is equivalent to keeping the source at position (0,0) and scanning the detection point on the grid described above. Ten scans

were performed and the displacement fields averaged to reduce the measurement noise. The raw (averaged) data corresponding to the in-phase and quadrature components of the displacement field are shown in Figs. 4(a) and 4(b), respectively. In the raw data, the displacement is dominated by the lower order, high spatial frequency modes: primarily the lowest order antisymmetric (A_0) and symmetric (S_0) modes. For these modes, the wave fronts appear to emanate from the detection point (0,0) on pth_1 and continue to diverge past the interface in pth_2. As expected, there is no evidence of backward wave propagation or associated negative refraction.

The S_2 (pth_1) and S_{2b} (pth_2) modes can be isolated from the other modes based on wave-number. The raw data was low pass filtered as follows: we performed a two- dimensional spatial Fourier transform on the image, multiplied this by a Gaussian image with a half-maximum intensity point of k_c = 16 mm^{-1}, and performed an inverse Fourier transform. This procedure leaves only the S_2 and S_{2b} modes whose wave-numbers lie below the filter cut-off (see Fig. 3). The filtered images are shown in Fig. 5. The in-phase and quadrature components of the displacement field are shown in Fig. 5(a) and Fig. 5(b), while the magnitude and phase are given in Fig. 5(c) and Fig. 5(d), respectively. As in Fig. 4, the waves appear to emanate from the detection point (0,0) on pth_1 which supports only the forward propagating S_2 in this region of $\omega(k)$ space. Upon mode conversion and transmission through the interface, however, the situation is quite different. The wave exhibits negative refraction and the diverging wave-fronts in pth_1 are converted to converging wave-fronts in pth_2 in association with the S_2 to S_{2b} mode conversion at the interface. Lamb wave focusing, consistent with that expected for a Veselago type lens, is

clearly observed in the images. For a given material attenuation rate, the attenuation per unit distance that a Lamb wave propagates is inversely proportional to the group velocity,[23] and it is believed that strong attenuation in the displacement field with distance from the interface observed in Fig. 5(c) is associated with the low group velocity (0.83 km/s) of the S_{2b} mode at 28 MHz.

V. DISCUSSION AND CONCLUSIONS

The characteristics of the lens require further discussion. First, the aperture of the lens appears to be limited to approximately 3.5 mm, and there appears to be little S_2 to S_{2b} mode conversion beyond a half angle of about 40^0. It is believed that this is a result of the redistribution of the Lamb wave energy into different modes to satisfy the continuity conditions at the interface. The interaction of Lamb waves with an interface is a complex process, and it is possible that the numerical aperture could be increased using different types of interfaces or alternate material systems. The wavelengths of the S_2 and S_{2b} modes were nearly matched at 28.0 MHz indicating that for an ideal Veselago lens the detection point and focal point should occur at equidistant points from the interface or, in the coordinate system shown in Fig. 5, the focal point should be at y = 4.0 mm. In the experimental result, the focal point appears to be shifted back from the interface. Spatial averaging Fig. 5(c) over 0.5 mm increments along the y axis, we find a minimum central lobe between y = 4.5 and y = 5.0 mm with a full width at half maximum of 0.6 mm; close to the wavelength of the S_{2b} mode (612 μm). We note that there are significant spatial fluctuations observed in the magnitude plot. While the origin of the signal distortion and extended focus are not clear, we propose that the former could stem from small

imperfections at the interface and non-uniformity in the amplitude of the S_2 to S_{2b} mode converted wave, while the latter may result from variations in the thickness of pth_1 or pth_2 over the imaged region. Nevertheless, it is somewhat remarkable that a Lamb wave lens can be created by a simple thickness step in a homogeneous, isotropic plate.

While the existence of backward waves in acoustic waveguides has been known for quite some time, there has been little work in the design of guided wave structures and sources which take advantage of this intriguing phenomenon. Here we have demonstrated that Lamb wave energy can be focused through mode conversion between forward and backward propagating waves at an interface. A modulated point source has been used for excitation, thereby exciting numerous modes in the system and exciting the mode of interest with low efficiency. Selective excitation of a single propagating mode can potentially be achieved, for example, through patterning the source function to match the periodicity of the desired mode at a particular frequency. Using this approach, and optimizing the interface for mode conversion between forward and backward propagating modes, it may be possible to fabricate an efficient high numerical aperture surface acoustic wave or Lamb wave lens. Ultimately, one could envision utilizing backward waves, negative refraction, and focusing effects in plates or thin films to manipulate the flow of acoustic energy in novel ways, with potential applications in acoustic wave devices or sensors, or in the nondestructive characterization of materials.

ACKNOWLEDGEMENTS

This work was partially funded by the National Science Foundation through Grant No. CMMI 0448796 and IIP 0712496.

References

1. V.G. Veselago, Sov. Phys. Usp. **10**, 509 (1968).

2. V. G. Veselago and E. E. Narimanov, Nat. Mater. **5**, 759 (2006).

3. S. A. Ramakrishna, Rep. Prog. Phys. **68**, 449 (2005).

4. C. M. Soukoulis, M. Kafesaki, and E. N. Economou, Adv. Mater. **18**, 1941 (2006).

5. H. Lamb, Proc. London Math. Soc. **1**, 473 (1904).

6. R.A. Shelby, D.R. Smith, and S. Schultz, Science **292**, 77 (2001).

7. A.A. Houck, J.B. Brock, and I.L. Chuang, Phys. Rev. Lett. **90**, 137401 (2003).

8. N. Fang D. Xi, J. Xu, M. Ambati, W. Srituravanich, C. Sun, and X. Zhang, Nat. Mater. **5**, 452 (2006).

9. J. Li and C.T. Chan, Phys. Rev. E **70**, 055602 (2004).

10. S. Zhang, L. Yin, and N. Fang, Phys. Rev. Lett. **102**, 194301 (2009).

11. M. Notomi, Phys. Rev. B **62,** 10696 (2000).

12. E. Cubukcu, K. Aydin, E. Ozbay, S. Foteinopoulou, and C.M. Soukoulis*.,* Nature **423**, 604 (2003).

13. S. Yang, J.H. Page, Z. Liu, M.L. Cowan, C.T. Chan, and P. Sheng*,* Phys. Rev. Lett. **93**, 024301 (2004).

14. M. Ibanescu, S.G. Johnson, D. Roundy, C. Luo, Y. Fink, and J.D. Joannopoulos, Phys. Rev. Lett. **92**, 063903 (2004).

15. A.H. Meitzler, J. Acoust. Soc. Am. **38**, 835 (1965).

16. I. Tolstoy and E. Usdin, J. Acoust. Soc. Am. **29**, 37 (1957).

17. S.D. Holland and D.E. Chimenti, Appl. Phys. Lett. **83**, 2704 (2003).

18. C. Prada, O. Balogun, and T.W. Murray, Appl. Phys. Lett. **87**, 194109 (2005).

19. D. Clorennec, C. Prada, and D. Royer, J. Appl. Phys. **101**, 034908 (2007).

20. P.L. Marston, J. Acoust. Soc. Am. **113**, 2659 (2003).

21. A.A. Maznev and A.G. Every, Appl. Phys. Lett. **95**, 011903 (2009).

22. J.D. Achenbach, *Wave Propagation in Elastic Solids* (North-Holland, Amsterdam, 1980).

23. A. Viktorov, *Raleigh and Lamb Waves* (Plenum, New York, 1967).

24. A.L. Shuvalov and O. Poncelet, Int. J. Solids Struct. **45**, 3430 (2008).

25. C. Prada, D. Clorennec, and D. Royer, J. Acoust. Soc. Am. **124**, 203 (2008).

Figure Captions

Figure 1. (a) Lamb wave dispersion curves in an aluminum plate of infinite extent and thickness h, with longitudinal and shear wave velocities of 6420 m/s and 3040 m/s, respectively. (b) A schematic of the plate with a step change in thickness. (c) Symmetric modes on each side of the thickness step and (d) a zoomed in theoretical (solid lines) and experimental plot of the dispersion curve in the vicinity of the crossing point between the S_2 and S_{2b} modes on the thick and thin sides of the plate.

Figure 2. Schematic showing the experimental setup. The detection point is fixed on the plate surface and the source is scanned using the translation stage.

Figure 3. Magnitudes of the Fourier transforms of the displacement measured as a function of distance, at a frequency of 28.0 MHz, with the source and receiver on the same side of the interface where (a) corresponds to the thick side of the plate (pth_1) and (b) the thin side (pth_2). The Lamb wave modes associated with each spatial frequency peak are labeled on the plot.

Figure 4. The in phase (a) and quadrature (b) components of the normal surface displacement measured with the detector fixed at x = 0 and y = 0, and the source scanned. The interface, located at y = 2.0 mm, is marked by arrows.

Figure 5. Images of only the low spatial frequency modes resulting from applying a low pass filter with a cut-off wave number of 16 mm^{-1} to the data shown in Figure 4. The in-phase and quadrature components of the normal surface displacement are shown in (a) and (b), while the magnitude and phase are given in (c) and (d), respectively. The interface, located at y = 2.0 mm, is marked by arrows.

FIGURE 1

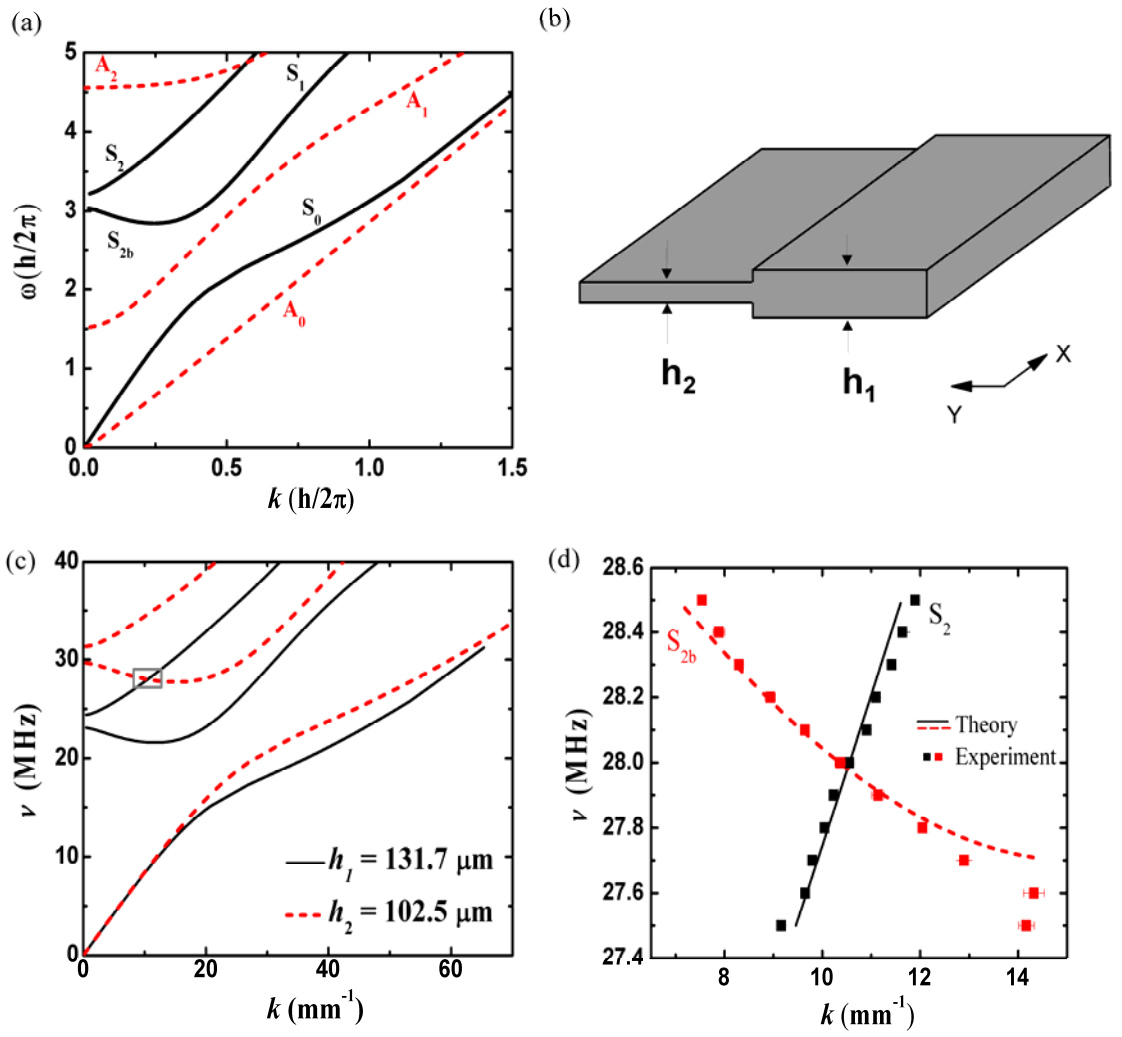
(a)
A2
S1
A1
S2
S0
S2b
A0
ω(h/2π)
k (h/2π)
(b)
h2
h1
X
Y
(c)
ν (MHz)
h1 = 131.7 μm
h2 = 102.5 μm
k (mm-1)
(d)
S2b
S2
Theory
Experiment
ν (MHz)
k (mm-1)

FIGURE 2

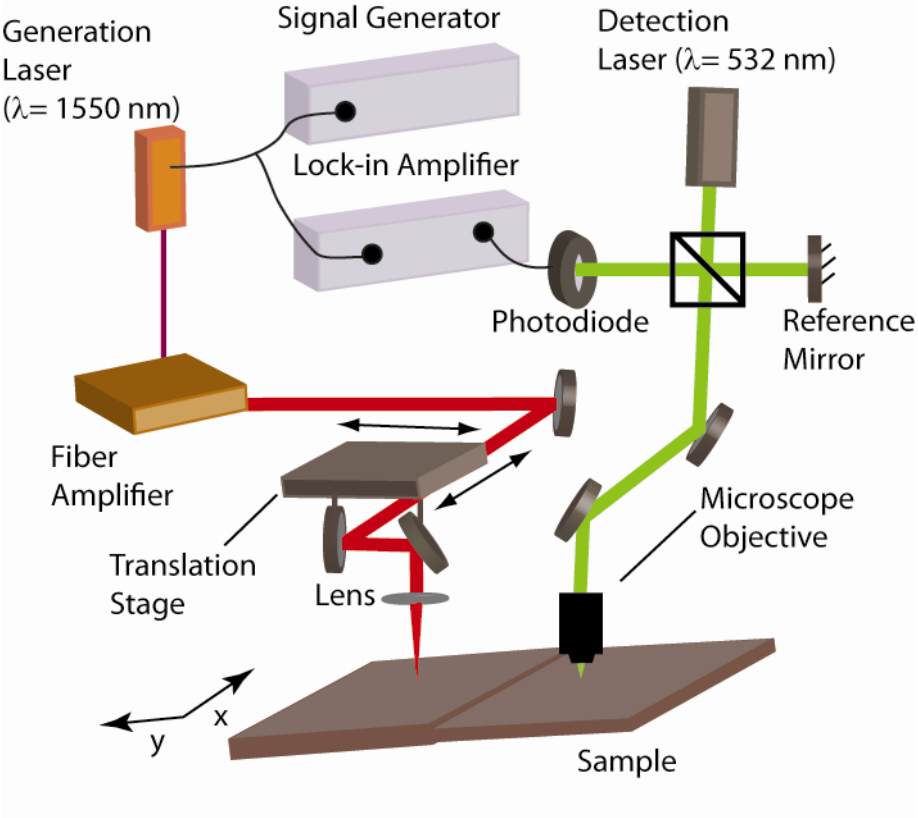
Generation
Laser
(λ= 1550 nm)
Signal Generator
Lock-in Amplifier
Detection
Laser (λ= 532 nm)
Photodiode
Reference
Mirror
Fiber
Amplifier
Translation
Stage
Lens
Microscope
Objective
x
y
Sample

FIGURE 3

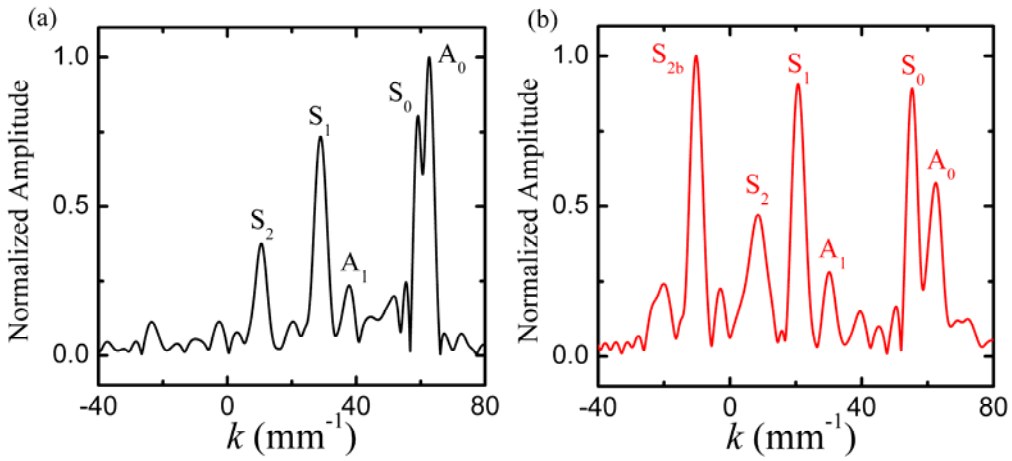
(a)
Normalized Amplitude
1.0
0.5
0.0
-40
0
40
80
k (mm-1)
S2
S1
A1
S0
A0
(b)
Normalized Amplitude
1.0
0.5
0.0
-40
0
40
80
k (mm-1)
S2b
S2
S1
A1
S0
A0

FIGURE 4

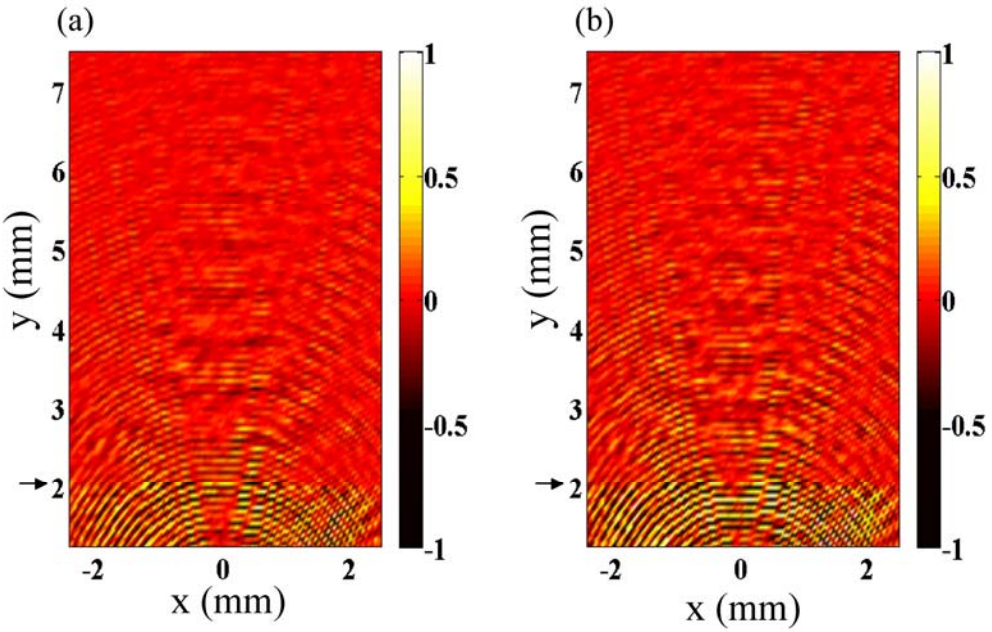

Color scale: Normalized Amplitude

FIGURE 5

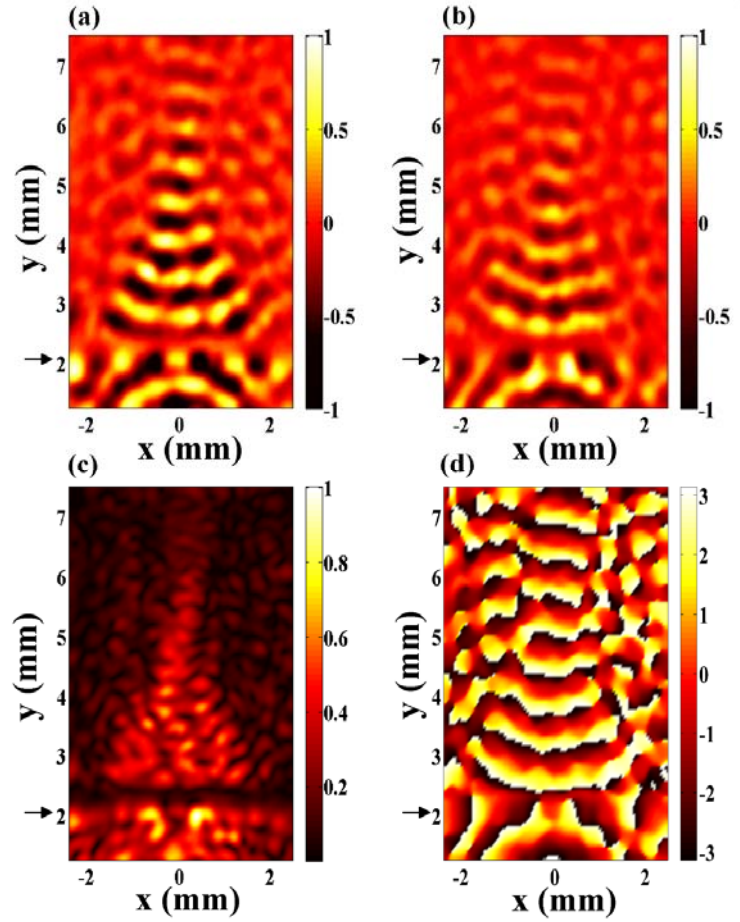
(a)
(b)
(c)
(d)
y (mm)
x (mm)
Color scale: (a)-(c) normalized amplitude and (d) phase (radians)